Changes in satellite-derived vegetation growth trend in China from 2002 to 2010

Juan Gu[*a], Xin Li[b], Chunlin Huang[b]
a,Center for Dryland Water Resources Research and Watershed Science, MOE Key Laboratory of Western China's Environmental Systems, Lanzhou University, Lanzhou, Gansu 730000, China
b,Cold and Arid Region Environmental and Engineering Research Institute, Chinese Academy of Science, Lanzhou, Gansu 730000, China

ABSTRACT

Net primary production (NPP) is the production of organic compounds from atmospheric or aquatic carbon dioxide, principally through the process of photosynthesis. Climate changes of this magnitude are expected to affect the NPP of the world's land ecosystems. In this study, we used a light-use efficiency model and linear regression model to describe and analyze the spatial and temporal patterns of terrestrial net primary productivity (NPP) in China during 2002-2010.

First, we used the reconstructed 16-day 0.05°MODIS NDVI product (MOD13C1), 0.05°gridded GLDAS (Global Land Data Assimilation System) meteorological data and land use map to estimate the NPP in China. The spatial variability of NPP was analyzed during all periods, growing seasons and different seasons, respectively. Based on regression analysis method, we quantified the trend of NPP change in China during 2002-2010.

Keywords: Trend, NPP, light use efficiency model, China

1. `INTRODUCTION

Net primary productivity (NPP) is the amount of solar energy converted to chemical energy through the process of photosynthesis (production minus respiration) and represents the primary source of food for Earth's heterotrophic organisms including human beings. Quantitative investigations on the NPP change, net ecosystem productivity (NEP) and net biosphere productivity (NBP) are important in the context of earth system science and global change studies (Ruimy, 1994).

Monitoring global terrestrial net primary production (NPP) is relevant to understanding the global carbon cycle and evaluating effects of interannual climate variation on food and fiber production (Running et al., 1999). Model simulation have been widely used to estimate NPP in global and regional vegetation monitoring. According to the calculation theory, the NPP model can be classified into the three types (Ruimy, 1994): climate-related models, process-based ecosystem models and remote sensing data-based light use efficiency model.

The remote sensing-based approach employs satellite-borne sensors to monitor NPP that achieve daily coverage over the Earth's surface at spatial resolutions of 250-1000m, such as the Moderate Resolution Imaging Spectroradiometer (MODIS). Surface reflectances derived from these sensors are used to infer the fraction of incoming photosynthetically active radiation absorbed by the vegetation (fAPAR). The combination of fAPAR and an estimate of incident PAR can provide an estimate of PAR absorbed by the canopy (APAR). Knowledge of the efficiency with which vegetation converts APAR into biomass then permits an estimate of NPP.

Recent climatic changes have enhanced plant growth in northern mid-latitudes and high latitudes. However, the description of the current changes of vegetation productivity in China has not before been expressed. In our study, we estimated the Chinese terrestrial NPP during the past decade by integrating remote sensing data, ground meteorological data and other vegetation eco-physiological data. In this paper, we describe the methods, data sources, and NPP estimates. Finally, we show the preliminary results of the spatial pattern of NPP.

[*] gujuan@lzu.edu.cn; phone 86 931 8910180; fax 86 931 8910180;

Remote Sensing for Agriculture, Ecosystems, and Hydrology XIV, edited by Christopher M. U. Neale, Antonino Maltese,
Proc. of SPIE Vol. 8531, 85310W · © 2012 SPIE · CCC code: 0277-786/12/$18 · doi: 10.1117/12.974313

2. DATA AND METHODS

In order to confirm the spatio-temporal variations observed in simulated NPP, we used the following data sets: air temperatures, precipitation, NDVI, and incident solar radiation. Here we provide a brief description of each of the independent data sets. Due to the different data sources in this study, we re-sampled the data with 1km resolution in order to better describe the characteristics of the vegetation in local-scale.

2.1 NPP model

Figure 1 illustrate the estimates of net primary productivity simulated by adjusted light use efficiency model Zhu(2005). The model can be characterized in three ways. (i) The computation of the water restriction factor is relatively easy and simple. It is driven with ground meteorological data and remote sensing data, and the complex soil parameters are avoided. (ii)The vegetation types and their classification accuracy are introduced to the computation of some key vegetation parameters, such as the maximum value of NDVI and the simple ratio (SR). This can remove some noise from the remote sensing data and the statistic errors of vegetation classification. (iii) The maximum light use efficiency (LUE) is simulated based on the observed NPP data in order to get more reasonable estimation of Chinese vegetation.

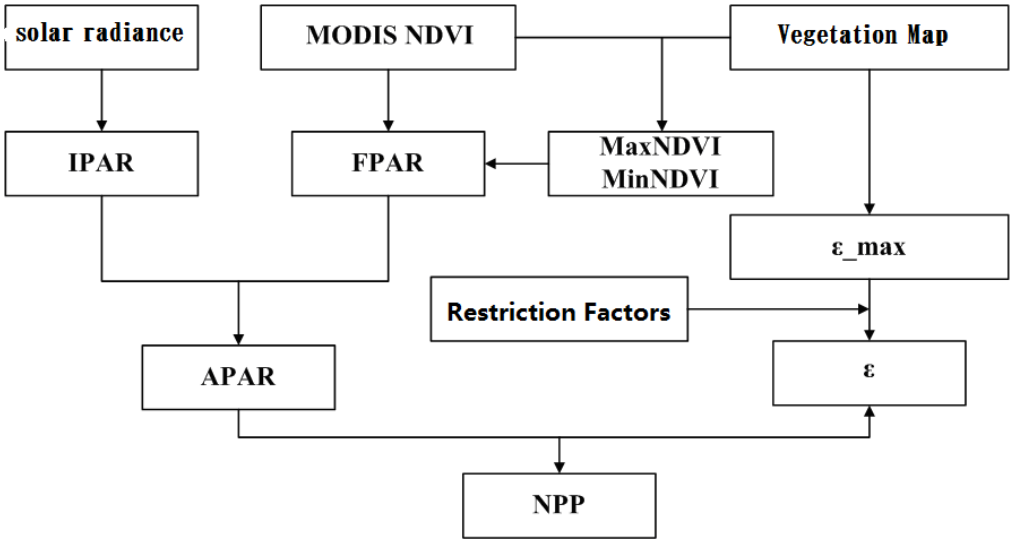

Figure 1. Components of NPP model (Zhu et al., 2005)

2.2 Radiation use efficiency

Radiation use efficiency (RUE, ε) is approximated on which climatic conditions have only slight influence. However, the water availability and temperature are considered as the important growth-limiting environmental factors by adjusting the photosynthesis of vegetation, which shows a strong spatial variation in large regions (Ruimy et al., 1994 ; Goetz et al., 1999 ; Turner et al., 2003). In our paper, the effects of temperature and water constraints are partially given by T_ε and P_ε respectively (Potter et al., 1993).

$$\varepsilon(x,t) = T_{\varepsilon 1}(x,t) \times T_{\varepsilon 2}(x,t) \times W_\varepsilon(x,t) \times \varepsilon_{\max} \tag{1}$$

where $T_{\varepsilon 1}(x,t)$ and $T_{\varepsilon 2}(x,t)$ are the influence factor of low temperature and high temperature stress to RUE, $W_\varepsilon(x,t)$ is the influence factor of water stress to RUE , $\varepsilon_{\max}$ is the maximum RUE.

$$T_{\varepsilon 1}(x,t) = 0.8 + 0.02 \times T_{opt}(x) - 0.0005 \times [T_{opt}(x)]^2 \tag{2}$$

where $T_{opt}(x)$ is the optimum temperature (correspond with the maximum NDVI), $T_{opt}(x)$ is defined zero when the mean monthly temperature ($T(x,t)$) is less than and equal to zero. $T_{\varepsilon 2}(x,t)$ is the change of RUE with temperature (Field et al., 1995):

$$T_{\varepsilon 2}(x,t) = \frac{1.184}{1+\exp[0.2\times(T_{opt}(x)-10-T(x,t))]} \times \frac{1}{1+\exp[0.3\times(-T_{opt}(x)-10-T(x,t))]} \tag{3}$$

$W_{\varepsilon}(x,t)$ ranges from 0.5 to 1 and calculated by the following (Piao et al., 2001)

$$W_{\varepsilon}(x,t) = 0.5 + 0.5\times E(x,t)/E_p(x,t) \tag{4}$$

$$E_p(x,t) = \frac{[E(x,t)+E_{p0}(x,t)]}{2} \tag{5}$$

where $E(x,t)$ is the actual regional evaporation (mm) and calculated by（Zhou et al., 1996）

$$E(x,t) = \frac{P(x,t)\times R_n(x,t)\times[P_2(x,t)+R_n{}^2(x,t)+P(x,t)\times R_n(x,t)]}{[P(x,t)+R_n(x,t)]\times[P^2(x,t)+R_n{}^2(x,t)]} \tag{6}$$

$$R_n(x,t) = \sqrt{E_{po}(x,t)\times P(x,t)}\times 0.369 + 0.598\times\sqrt{\frac{E_{p0}(x,t)}{P(x,t)}} \tag{7}$$

$E_p(x,t)$ is potential evaporation (mm) (Zhou et al., 1996):

$$E_p(x,t) = \sqrt{E(x,t)+E_{p0}(x,t)} \tag{8}$$

Where $E_{p0}(x,t)$ is obtained by Thornthwaite vegetation-climate model。

$$E_{po}(x,t) = 16\times[\frac{10\times T(x,t)}{I(x)}]^{a(x)} \tag{9}$$

$$a(x) = [0.6751\times I^3(x) - 77.1\times I^2(x) + 17920\times I(x) + 492390]\times 10^{-6} \tag{10}$$

$$I(x) = \sum_{t=1}^{12}[\frac{T(x,t)}{5}]^{1.514} \tag{11}$$

Where I(x) is the total heat index of one year, $a(x)$ can be calculated by the above equation when the temperature ranges in[0℃ , 26.5℃]. And $E_{p0}(x,t)$ is adjusted by the actual day length and the days of month. Then the possible evaporation (APE(x,t)) can be calculated by:

$$APE(x,t) = E_{p0}(x,t)\times CF(x,t) \tag{12}$$

In our study, the maximum light use efficiency of all biomes is referenced from the observation.

Table 1 the value of monthly maximum light use efficiency in the model (Zhu,2005)

Code	Biome types	Monthly maximum Light use efficiency (gC/MJ)
1	needleleaved deciduous forest	0.485
2	needleleaved evergreen forest	0.389
3	broadleaved evergreen forest	0.985
4	broadleaved deciduous forest	0.692
5	bush	0.429
6	sparse woods	0.475
7	seaside wet lands	0.542
8	alpine and sub_alpine meadow	0.542
9	slope grassland	0.542
10	plain grassland	0.542
11	desert grassland	0.542
12	meadow	0.542
13	city	/
14	river	/
15	lake	/
16	swamp	0.542
17	glacier	/
18	bare rocks	/
19	gravels	/
20	dersert	/
21	farmland	0.542
22	alpine and sub-alpine plain grass	0.542

2.3 MODIS NDVI reconstruction

The input NDVI data used in the model is reconstructed MODIS NDVI (MOD13A2) based on a simplified data assimilation scheme (Figure 2). Since the current NDVI product is still spatio-temporally discontinuous due to cloud cover, seasonal snow, atmospheric variability, bi-directional effects and instrument problems (Huete and Liu,1994; Huete, 1999; Xiao et al., 2003). More detail of the reconstruction algorithm can be obtained in Gu (2009).

MOD13A2 products are 16-Day L3 Global 1 km SIN Grid VI data sets, which include two vegetation index types (NDVI and EVI). In this paper, MOD13A2 products covering China were acquired for the period of interest (2002–2010). During the process of NDVI data reconstruction, NDVI QA data are used to determine the weight required by the data assimilation method for every time step.

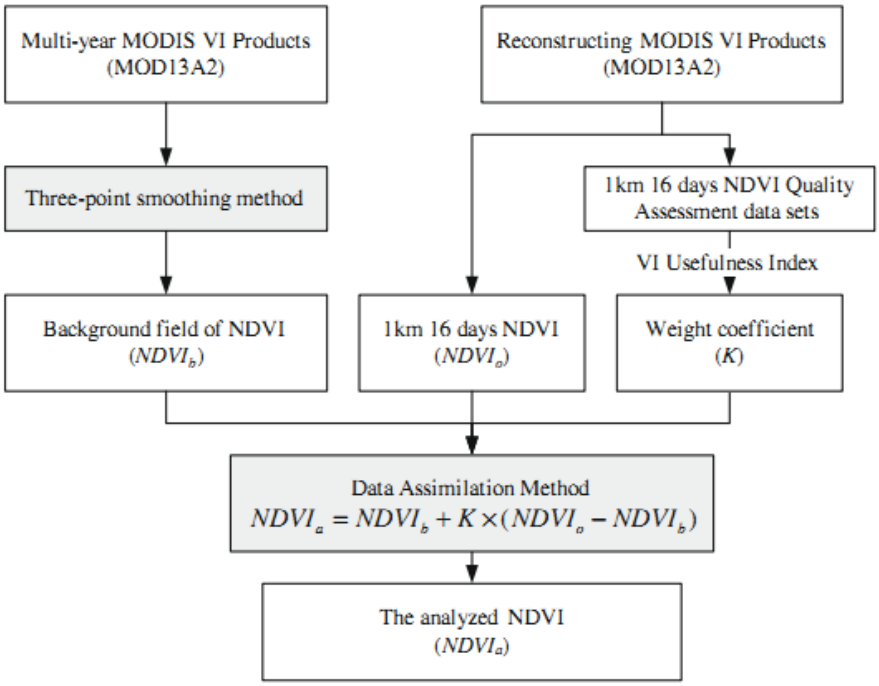

Figure 2. A flowchart outlining the reconstruction process of MODIS NDVI data

2.4 The basic biomes used in the model

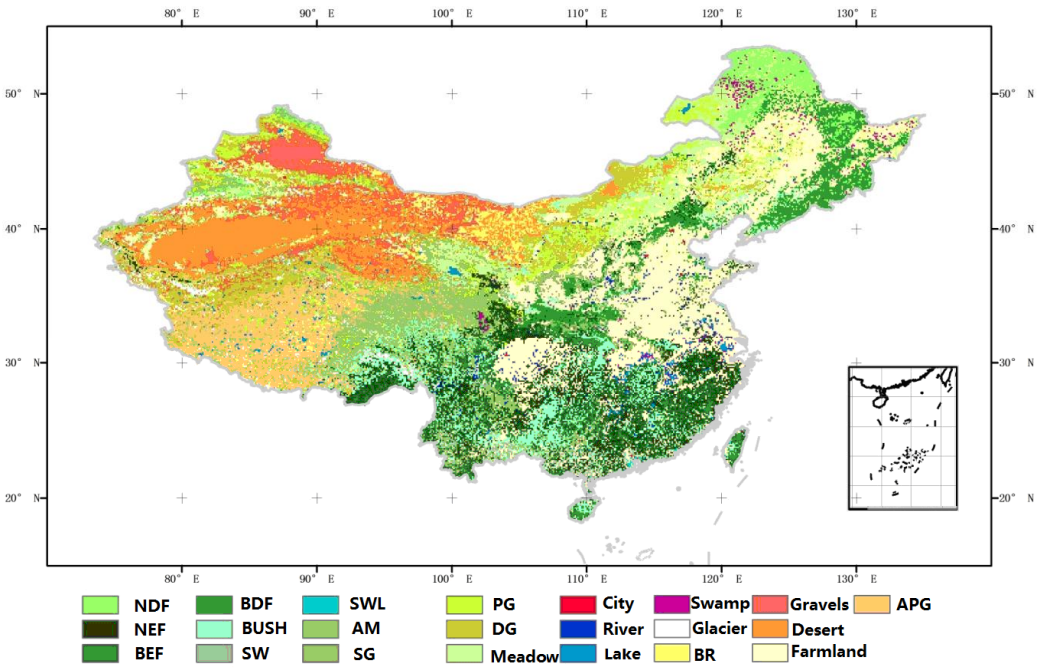

Figure 3. The basic biomes for China

The biomes were classified in the vegetation map into 22 types (Figure 3) based on the vegetation maps of three period (1996, 2000, 2003), which include needle leaved deciduous forest (NDF), needle leaved evergreen forest (NEF), broadleaved evergreen forest(BEF), broadleaved deciduous forest (BDF), bush, sparse woods (SW), seaside wet lands (SWL), alpine and sub-alpine meadow (AM), slope grassland (SG), plain grassland (PG), desert grassland (DG),

meadow, city, river, lake, swamp, glacier, bare rocks (BR), gravels, dessert, farmland, alpine and sub-alpine plain grass (APG). This biome types fall into three main categories: forests, grassland (include grass and savanna) and tundra, with spatial distribution patterns that largely agree with the three general climate zones in China (the eastern monsoon zone, the north-west arid zone, the Tibetan Plateau frigid zone).

2.5 GLDAS data

The grided total solar radiation, temperature and precipitation data with 0.25° resolution are derived from the GLDAS data product and then resampled for our model. GLDAS data set include global time series of land surface water and energy cycle variables which was simulated by the Global Land Data Assimilation System (GLDAS; http://ldas.gsfc.nasa.gov/) driving the Noah land surface model (LSM). The project is led by scientists at NASA Goddard Space Flight Center and funded by NASA's Energy and Water Cycle Study (NEWS) Program (http://wec.gsfc.nasa.gov/). GLDAS datasets are available from the NASA Goddard Earth Sciences Data and Information Services Center (GES DISC).

2.6 Accuracy assessment

In order to make an assessment of our model results, we compared other model output with respect to the annual NPP for the land biosphere of China. Results show that the NPP values are in agreement with the measured and other model outputs in different vegetation types, proving that the NPP model is appropriate for simulating NPP of the China (Table 2).

Table 2 Comparison of simulated and measured NPP values of different ecosystems in China (Zhu, 2005; Gao, 2008)

Type	CEVSA	CASA	GLOPEM	GEOLUE	GEOPRO	value	observation
needleleaved evergreen forest	358	464	355	586	249	249-586	179-806
broadleaved evergreen forest	718	561	718	1086	622	561-1086	407-1913
needleleaved deciduous forest	352	498	367	657	268	268-657	179-824
broadleaved deciduous forest	472	515	451	565	316	316-565	114-1669
Bush	700	492	616	723	561	492-723	/
Grassland	208	245	145	178	168	145-245	/
Farmland	577	362	474	372	344	344-577	/
Unused land	33	69	32	23	20	20-69	/

3. PRELIMINARY RESULTS

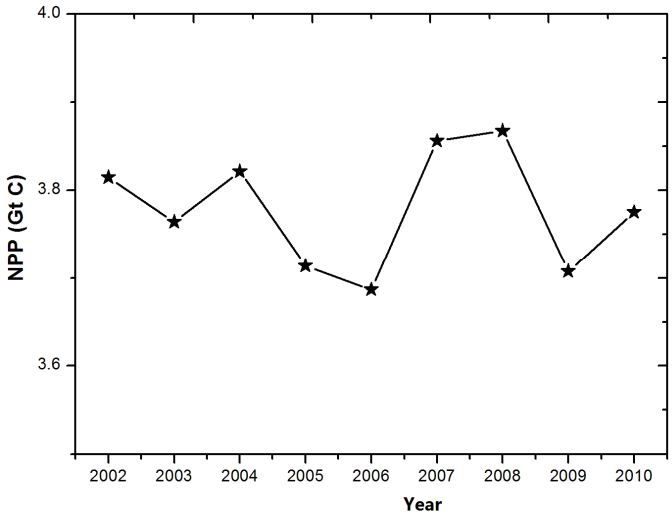

Figure 4. The estimate of annual NPP for a spanning time period of 9 years

As Figure 4 shows, the mean NPP of terrestrial vegetation in China is 3.68 GtC/a from 2002 to 2010. The total NPP ranges from 3.86 GtC/a to 3.68 GtC/a, and the average value is 3.78 GtC/a. The NPP decreased with the ratio of 0.03 during the period from 2002 to 2006, and there is no significant change feature from all study period (R^2=0.004 , P<0.01) . The maximum NPP value is in 2008, and the minimum is in 2006.

There are clearly strong regional variations in Chinese terrestrial vegetation NPP. It decreased from Southeast China toward the northwest. Regions of higher productivity are found in the Southern Hainan Island, Southwestern Yunnan and Southeast Tibet, whereas the western China has very small NPP values. The vertical variation of NPP is also obvious with the altitude change. As Figure 5-8 shows, the estimate of the total annual terrestrial NPP is about 3.78 Gt C/a in China during 2002-2010, the spring terrestrial NPP is about 0.64Gt C/a, the autumn terrestrial NPP is about 1.59Gt C/a, and the summer terrestrial NPP is about 0.81Gt C/a.

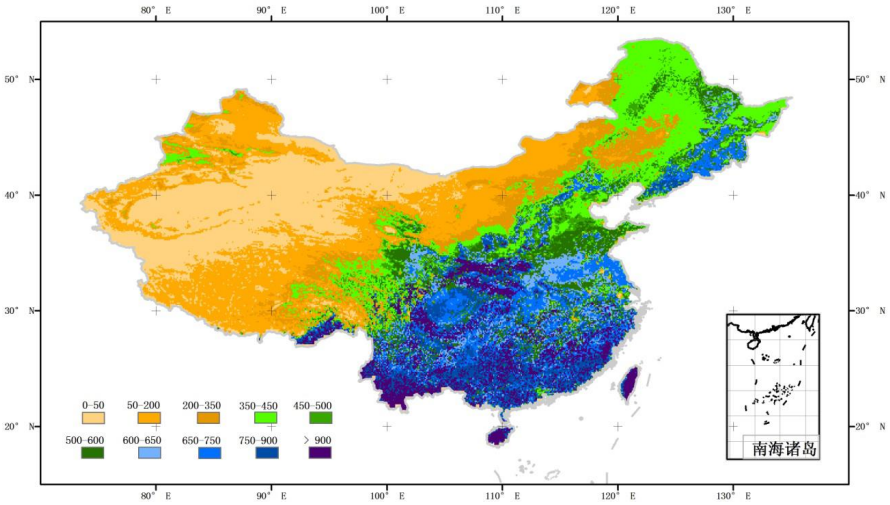

Figure 5. Spatial pattern of Chinese terrestrial vegetation NPP (unit：gC/m2·a)

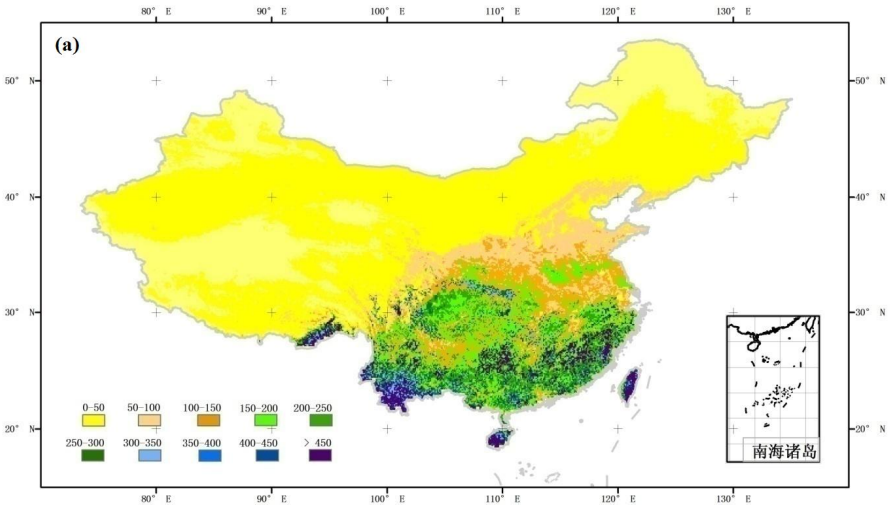

Figure 6. Spatial pattern of Chinese terrestrial vegetation NPP in spring (unit：gC/m2·a)

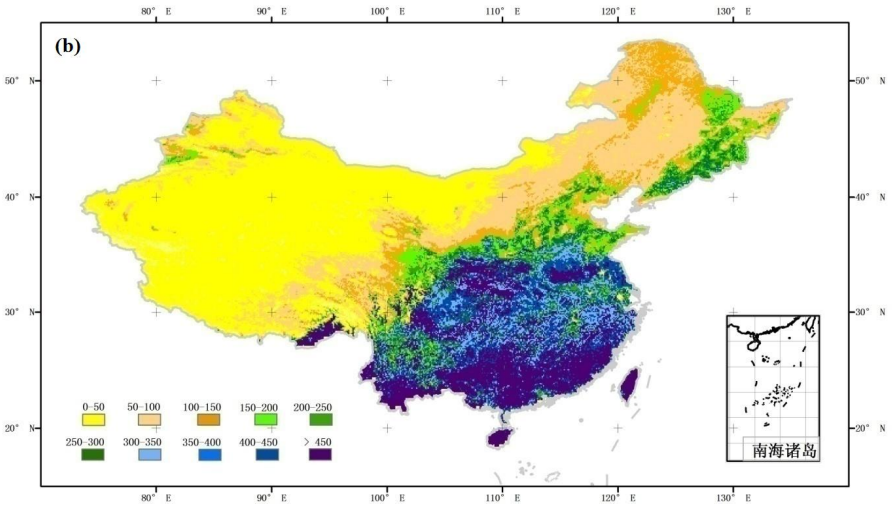

Figure 7. Spatial pattern of Chinese terrestrial vegetation NPP in summer (unit：gC/m2·a)

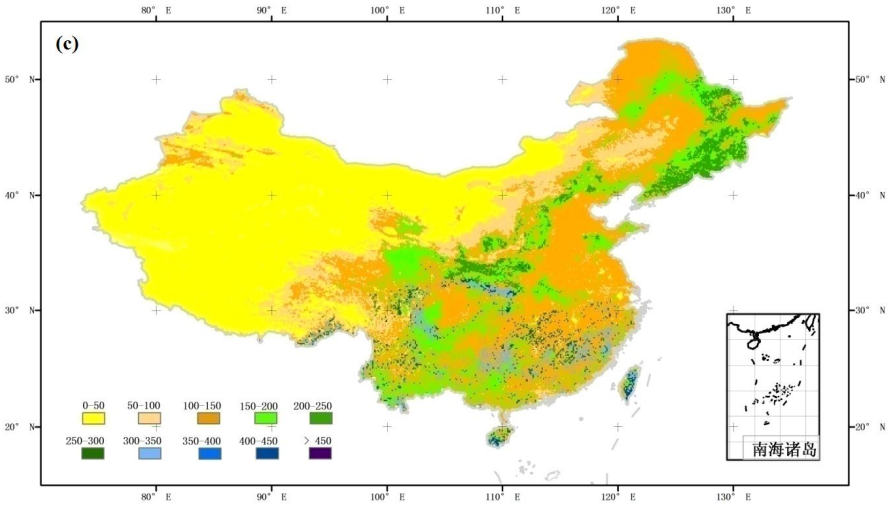

Figure 8. Spatial pattern of Chinese terrestrial vegetation NPP in autumn (unit：gC/m2·a)

We also performed the regression analysis for the trend of NPP in China. Most part of China change significantly around 2004 or 2006 due to climate change, which include the north part of Xinjiang, the east part of Inner Mongolia and the southeast part of Qinghai Tibet Plateau. The NPP in growing season showed an increasing trend during 2002-2010. 26.6% of the total area was increasing and 21% was decreasing. In spring, 14.5% of the total area was increasing and 10.4% was decreasing. In summer, 19.5% of the total area was increasing and 17.1% was decreasing. In autumn, 21.4% of the total area was increasing and 19.6% was decreasing. It is noticeable that some little pixel groups distributed in the Central and East China have obvious decreasing trend. These areas are often located in the metropolises. This maybe results from the urbanization.

4. CONCLUSIONS

Our results indicate: (1) The NPP estimation based on remote sensing data is more reasonable for regional scale study. Specially, the reconstructed time-series MODIS NDVI data has been applied and improved the accuracy of NPP estimation by removing the noise. (2) The fundamental spatial pattern of annual NPP in China was characterized by high NPP levels distributed in the southeast and low NPP levels in the northwest which was likely due to difference of major climatic factors along latitude. In all vegetation types, the maximum annual NPP was observed on evergreen broadleaf. The high level NPP was distributed in the south part of Hainan province, the southwest part of Yunnan province, and the

southeast part of Qinghai-Tibet Plateau. The significant seasonal change feature was shown in all vegetation types in which the change amplitude of evergreen vegetation is the highest, and the desert is the lowest. (3) The whole forest ecosystems occupied the largest part of NPP in China (40.32%), then the farmland (24.30%), followed by grassland (10.32%). The desert occupied the lowest part of NPP in China (0.66%). (4) As a whole, the NPP was increasing in northwest China but decreasing in northeast China and southeast China.

REFERENCES

[1] Field, C. B., Randerson, J. T., Malmstrom, C. M. "Global net primary production: combining ecology and remote sensing". Remote Sensing of Environment. 51(1):74-88(1995)

[2] Gao Z.Q., Liu J.Y. "Comparison Study of Chinese terrestrial NPP" .Chinese Science Bulletin.53(3):317-326(2008)

[3] Gu J., Li X., Huang C. "A simplified data assimilation method for reconstructing time-series MODIS NDVI data". Advances in Space Research. 44,501-509(2009).

[4] Huete A. R., Justice C., Leeuwen V., 1999. "MODIS vegetation index algorithm theoretical basis document", Version 3, http://modis.gsfc.nasa.gov/data/atbd/land_atbd.html.

[5] Piao S.L., Fang J.Y., Guo Q.H. "Application of CASA model to the estimation of Chinese terrestrial NPP". Acta Phytoecologica Sinica. 25(5):603-608(2001).

[6] Ruimy, A., Saugier, B. "Methodology for the estimation of terrestrial net primary production from remotely sensed data". Journal of Geophysical Research. 97:18515-18521(1994).

[7] Running, S. W., Hunt, Jr. E. R., Generalization of a forest ecosystem process model for other biomes, BIOME-BGC, and an application for global-scale models, in Scaling Processes Between Leaf and Landscape Levels (eds. Ehleringer, J. R., Field, C.), San Diego: Academic Press, 141,(1993)

[8] Xiao, X.M., Zhang, B., Braswell, Q., et al. "Sensitivity of vegetation indices to atmospheric aerosols: continental-scale observations in Northern Asia". Remote Sensing of Environment. 84, 385–392(2003).

[9] Zhou G.S., Zhang X.S. "Study on NPP of natural vegetation in China under global climate change". Acta Phytoecologica Sinica. 20(1):11-19(1996)

[10] Zhu W.Q. "Estimation of NPP of Chinese terrestrial vegetation based on remote sensing and its relationship with global climate change". PhD thesis, Beijing Normal University (2005)

ACKNOWLEDGEMENT

This research was supported by One Hundred Person Project of the Chinese Academy of Sciences "multi-sensor hydrological data assimilation for key hydrological variables in cold and arid regions" (Grant number: 29Y127D01) and NSFC funding of Young Scientist (Grant number: 41101387/D010702).